at each frequency. Wide-band data over the short millimeter-wavelengths region, and detailed data around 100 GHz measured with a distance of 1 GHz are given in the figure. These data show the following: 1) wide-band detection over the 100–300-GHz region is obtained, and detection up to the submillimeter-wavelengths region can be expected; and 2) movable shorts employed are effective for wide-band tuning.

V. Conclusion

Circuit structure and performance of a wide band and mechanically stable quasi-optical detector for 100–300 GHz is discussed. The detector reported here is convenient for applications such as spectroscopy and radio astronomy over the short millimeter-wavelengths region. Moreover, this circuit technique is easily extended to submillimeter detection and mixing.

Acknowledgment

The authors wish to thank Dr. H. Kimura, Dr. M. Fujimoto, and Dr. M. Akaike for their valuable guidance and discussions.

References

[1] L. M. Matarrese and K. M. Evenson, "Improved coupling to infrared whisker diodes by use of antenna theory," *Appl. Phys. Lett.*, vol. 17, no. 1, p. 1, July 1970.
[2] K. Mizuno *et al.*, "Submillimeter detection using a Shottky diode with a long-wire antenna," *Appl. Phys. Lett.*, vol. 26, no. 11, p. 1, pp. 605–607, June 1975.
[3] S. Yuki *et al.*, "Millimeter-wave impatt oscillators and wideband detectors," *Tech. Group Microwaves, Inst. Electron. Commun. Eng. Japan*, vol. MW-75-58, Sept. 1975.
[4] H. Kato *et al.*, "A 200-GHz-output doubler," in *Proc. 1977 Nat. Conv. Inst. Electron. Commun. Eng. Japan*, vol. 3, p. 180, Mar. 1977.
[5] K. Yamamoto *et al.*, "200-GHz waveguide components," *Tech. Group on Electron. Measurements, Inst. Elect. Eng. Japan*, vol. EM-77-20, June 1977.

An Avalanching Optoelectronic Microwave Switch

RICHARD A. KIEHL, MEMBER, IEEE

***Abstract*—A new optoelectronic microwave switching device is described. The device is composed of a semiconductor junction diode that is incorporated into a transmission line and illuminated with optical pulses from a semiconductor laser. Switching of microwave signals is achieved by changes in the RF impedance of the diode's high-field region resulting from an optically induced switching between low- and high-level avalanche states.**

Experimental results demonstrating the switching characteristics and speed of this device are presented along with a basic theory of operation. The ultimate capabilities of this device and its advantages over conventional p-i-n diode switches and other optoelectronic switching devices are also discussed.

I. Introduction

THERE HAS BEEN recent interest in the use of optical techniques for the control of microwave signals. This interest has been stimulated by the need for faster switching of moderate- to high-power microwave signals for both high-speed digital microwaves and high-resolution radar systems. For such applications, optical techniques offer higher speeds than conventional diode-switching techniques (p-i-n diodes), which are hampered by basic power-speed limitations [1]. In addition, optical control techniques permit virtually complete isolation between the RF and modulator circuitry of a system, thus eliminating both the problem of spurious "modulation-circuit oscillation" of the RF source, and of radar desensitization due to RF leakage.

Two basic approaches for optical control of microwave signals are being investigated. The first is direct control [2]–[4] of the internal dynamics of a solid-state oscillator. In this approach, optical signals are used to generate free carriers within the active region of, for example, a TRAPATT diode oscillator. Control of the frequency and amplitude of the oscillations is achieved through the modification of the diode's oscillatory dynamics caused by the presence of these optically generated carriers. Similarly, optical control of the gain characteristics of solid-state amplifiers is also expected to be possible.

In the second approach, which has been followed in the work described here, the optical signal is used to control the RF impedance of an element placed in the microwave

Manuscript received May 12, 1978; revised October 30, 1978. This work was supported by the United States Department of Energy (DOE) under Contract AT(29-1)789.

The author is with Sandia Laboratories, Albuquerque, NM 87185. Sandia Laboratories is a United States Department of Energy Facility.

0018-9480/79/0500-0533$00.75 ©1979 IEEE

signal path. Optically induced changes in the element impedance result in changes in the power transmission, which allow switching and gating of microwave signals to be achieved. Devices of this type, proposed so far [5], [6] have been based upon the optical generation of semiconductor plasmas.

In the present paper, we describe a new optoelectronic switching device which utilizes an optically controlled carrier avalanche to produce microwave switching. A description of the device and its basic principle of operation is given in Section II. Experimental results demonstrating its switching characteristics and speed are presented in Section III. The ultimate capabilities of the device and its advantages over other switching devices are discussed in Section IV. Finally, conclusions are given in Section V.

II. Description and Principle of Operation

The device is composed of a semiconductor junction diode which is connected across a gap in a transmission line and illuminated with an optical signal emitted by a semiconductor laser, as shown in Fig. 1. The diode is reverse-biased at a constant level which is sufficiently high to produce a low-level avalanche of the carriers in the high-field region. A shunt element with admittance Y_p is included to resonate the diode's "depletion" capacitance at the desired operating frequency. Thus the impedance of the parallel combination is high in the absence of RF conduction through the high-field region. In contrast to conventional diode switches, which operate by an electrically induced switching between forward- and reverse-bias states, the physical mechanism utilized in this device is an *optically induced* switching between high- and low-level *avalanche* states, at constant bias. In the absence of light, the relatively depleted condition of the high-field region results in a high-impedance state. During an optical pulse, multiplication of optically generated carriers produces a low-impedance state. Following the termination of the optical pulse, carriers are quickly swept out of the high-field region by the dc bias field, causing the diode to rapidly return to its high-impedance state.

A. Switching Characteristics

The effect of such optically induced changes in the carrier avalanche on the RF impedance can be understood from a simple model describing carrier transport through an avalanche region under the assumptions that 1) both electrons and holes travel with the same saturated drift velocity v_s, 2) the field-dependent avalanche coefficient $\alpha(E)$ is the same for both carriers, and 3) the electric field is constant throughout the region of length l. Under these assumptions, the carrier-continuity equations can be combined [7] to obtain an equation for the total conduction current I of the form

$$\frac{l}{2v_s}\frac{dI}{dt}+I[1-l\alpha(E)]=I_s \tag{1}$$

where E is the electric field and I_s is the reverse saturation current. The dc solution to (1) is

$$I_0=\frac{1}{1-l\alpha(E_0)}I_s\equiv MI_s \tag{2}$$

where I_0 and E_0 are dc quantities and M has been defined to be the conventional avalanche multiplication factor.

For small amplitude ac perturbations, (1) becomes

$$\frac{j\omega l}{2v_s}\tilde{I}+[1-l\alpha(E_0)]\tilde{I}=l\alpha' I_0\tilde{E} \tag{3}$$

where tilde's denote phasor quantities and

$$\alpha'=\left.\frac{\partial\alpha}{\partial E}\right|_{E_0}.$$

Integration of (3) across the avalanche region and substitution from (2) then gives

$$Z_a(\omega)=\left(\frac{1}{\alpha' M^2}+j\frac{\omega l}{2\alpha' v_s M}\right)\frac{1}{I_s} \tag{4}$$

for the avalanche impedance Z_a.

From the above, it should be noted that Z_a is dependent on the dc bias condition through the multiplication factor M. Specifically, Z_a is lower at higher multiplication levels, i.e., higher bias levels. It is also apparent that Z_a decreases with increasing reverse saturation current I_s. In the present situation, I_s is the result of optical as well as the usual thermal generation of carriers. For a side-illuminated device, we take the optical generation rate G to be the average over the active area as given by

$$G=\frac{\Phi_0}{\sqrt{A}}(1-e^{-\beta\sqrt{A}}) \tag{5}$$

where A, Φ_0, and β are the device area, incident photon flux density, and optical absorption coefficient, respectively. Accordingly, I_s can be written

$$I_s=I_t+ql\sqrt{A}\,\Phi_0(1-e^{-\beta\sqrt{A}}) \tag{6}$$

where I_t is the reverse saturation current due only to thermal generation.

Equations (4) and (6) indicate that the impedance decreases when the device is illuminated, and that the level

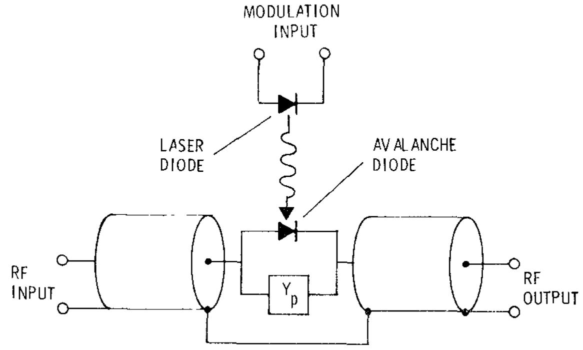

Fig. 1. Schematic diagram of an avalanching optoelectronic microwave switch. When the diode is illuminated by the semiconductor laser, multiplication of optically generated carriers results in high transmission. The shunt element Y_p serves to resonate the diode capacitance, resulting in low transmission in the absence of illumination.

of the dc bias affects the magnitude of both the on-state (illuminated) and off-state (unilluminated) impedances.

In order to see what this dependence of impedance on bias and illumination means in terms of switching behavior, we take the diode to be mounted as shown in Fig. 1. For a matched system with a characteristic resistance R_0 equal to 50 Ω, the dc and field in the avalanche region are related to the dc supply voltage V_B by

$$V_B = lE_0 + 2R_0 I_0. \tag{7}$$

In addition to the avalanche impedance Z_a, the diode introduces a capacitance (its "depletion" capacitance) across the transmission line gap. The shunt element Y_p is chosen such that its susceptance B_p parallel-resonates this capacitance at the desired operating frequency. Thus the total gap impedance Z_g is equal to the parallel combination of the avalanche impedance Z_a and the conductance of the shunt element G_p. That is,

$$Z_g = \frac{Z_a}{1 + G_p Z_a}. \tag{8}$$

A nonzero shunt conductance is included to account both for losses in the shunt element and residual coupling across the gap. (The coupling contribution is actually reactive, but this makes little difference in terms of transmitted power.)

As a specific example, we will choose the model parameters to be typical of the experimental (but far from optimal) GaAs devices described later. Assuming a one-sided abrupt junction, the total depletion region length at breakdown l_t is found to be 1.3 μm for the $3\times10^{16}\text{-cm}^{-3}$ n-layer of these diodes. The effective avalanche region length l given by

$$\alpha l = \int_0^{l_t} \alpha \, dx$$

is, therefore, 0.3 μm. The values for A, I_t, and ω are 1.6×10^{-4} cm², 1 nA, and $(2\pi\times4.5)$ GHz, respectively. Optical and material parameters appropriate for GaAs at 904 nm and 300° K are employed. The value of G_p is taken to be 5×10^{-4} mho, and was chosen to give approximately −25-dB transmission across the gap with the diode removed, in correspondence with typical measured values.

The transmitted power P_t in the on- and off-states is determined by

$$P_i = P_t\left[\left(\frac{R_g}{2R_0}+1\right)^2 + \left(\frac{X_g}{2R_0}\right)^2\right] \tag{9}$$

where P_i is the incident power and R_g and X_g are the real and imaginary parts of the gap impedance, respectively. The on/off ratio of this device is the ratio of transmitted power during illumination to that with no illumination. Using the above model, the on/off ratio was determined from (9), and is shown in Fig. 2 as a function of the dc bias current (I_0 in the off-state) at various illumination levels. The figure shows that the on/off ratio is high at moderate bias currents and drops rapidly on either side of this range.

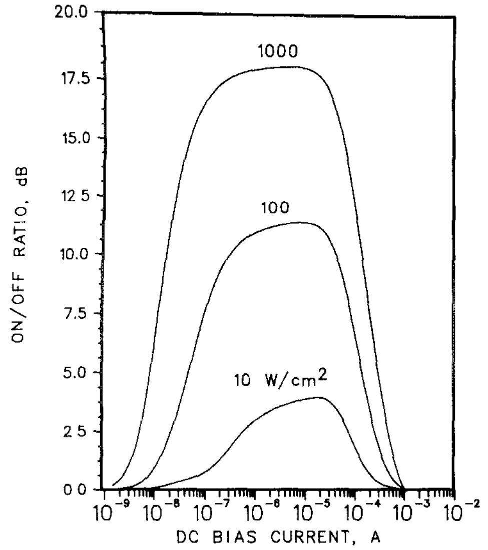

Fig. 2. Dependence of on/off ratio on bias current (off-state diode current) for various optical signal levels.

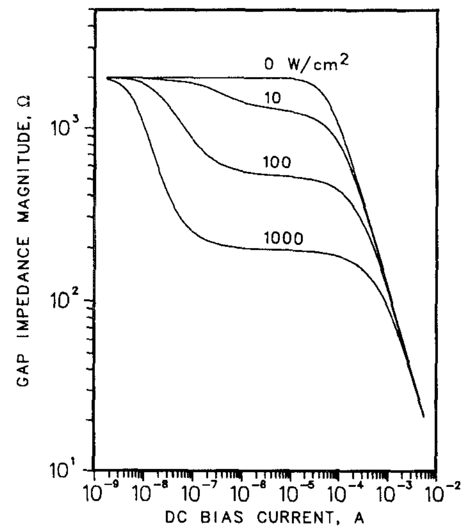

Fig. 3. Variation of gap impedance magnitude $|Z_g|$ with optical signal level as a function of bias current.

This peaking in the on/off ratio can be understood from Fig. 3 which shows the magnitude of the gap impedance for no illumination and for various illumination levels. At low biases, the impedance during illumination $|Z_g^{\text{on}}|$ and the impedance for no illumination $|Z_g^{\text{off}}|$ are nearly equal, since both are limited by G_p. Hence, at low bias, the on/off ratio is low. At moderate bias levels, $|Z_g^{\text{on}}|$ drops to a level much lower than $|Z_g^{\text{off}}|$, resulting in high transmission during the on-state and, accordingly, an increased on/off ratio. As the bias is increased still further, however, $|Z_g^{\text{off}}|$ also drops to a low level. Therefore, high transmission occurs during both states, again producing a low on/off ratio.

The foregoing results, for what is a quite unoptimized case, illustrate that high on/off-ratio microwave switching can be achieved by biasing the diode to a moderate level

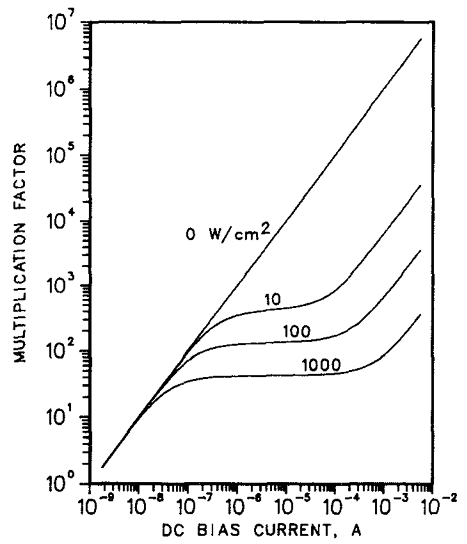

Fig. 4. Variation of the avalanche multiplication factor with optical signal level as a function of bias current.

of avalanche breakdown, and illuminating it at intensities within the limits of present semiconductor lasers. The fact that good performance can be obtained at very low bias currents is significant, since this means that the diode will have little tendency to exhibit electrical instability [8] due to avalanche transit-time effects.

B. Switching Speed

The switching speed or modulation rate of the device is limited by the time it takes the impedance to change from one state to another. One would expect that this will depend on the time it takes for the avalanche current to change in response to photo-induced changes in the reverse-saturation current. The avalanche response time can be determined from (1). For an optical signal composed of a dc component plus a small step change, I_s is of the form $I_s(t) = I_{s0} + I_{s1}u(t)$, where u is the unit step function. Solution of (1) gives

$$I(t) = M\left[I_{s0} + I_{s1}\left\{ 1 - \exp\left(\frac{-2v_s t}{Ml} \right) \right\} \right]. \qquad (10)$$

Hence, the response is characterized by the time constant $\tau = M(l/2v_s)$, or M times one-half the transit time through the avalanche region. The speed of the device will, therefore, be dependent on the level of avalanche multiplication.

Since the flow of diode current through the external resistance acts to reduce the field in the avalanche region, the level of multiplication that occurs for a given bias decreases with increased illumination in accordance with $M \sim 1/\sqrt{I_s}$ [9]. The switching speed will, therefore, be faster at higher illumination levels.

Fig. 4 shows the calculated multiplication factor as a function of bias for various illumination levels. For an illumination level of 1000 W/cm^2 and a bias on the order of 10 μA, which were the optimum conditions for high on/off ratio, it is seen that the multiplication factor is about 40. For a 0.3-μm avalanche region, this corresponds to a τ of 60 ps. Hence, we conclude that the limitation imposed by the avalanche response time at the multiplication levels needed for good performance is not severe, and high-speed switching should be possible.

III. Experimental Results

Both microstrip and coaxial configurations of the device have been tested experimentally. The diodes used for these experiments were Schottky-barrier GaAs mesa structures. The active semiconductor region was 5 mil in diameter and consisted of a 4-μm n-type epitaxial layer doped to 3×10^{16} cm^{-3} on an n$^+$ substrate. The avalanche voltage of the diodes was approximately 40 V. A microstrip version is shown in Fig. 5. In this device, the diode is mounted at the gap of a 50-Ω alumina microstripline. A series L–C circuit, connected in shunt with the diode, is provided by a 100-pF MOS capacitor and its connecting wire. The inductive reactance of the shunt element at the 4.5-GHz operating frequency serves to resonate the diode capacitance, thus producing a notch in the transmitted power over a 100-MHz 3-dB bandwidth. Side illumination of the diode is achieved by a fiber-coupled pulsed 10-W GaAs laser emitting at 904 nm. The GaAs laser was driven with an avalanche-transistor pulse circuit.

The measurement apparatus used in the experiments is shown in Fig. 6. Electrical bias was provided by an HP11590A insertion unit with the dc return provided by a 3-dB attenuator placed on the output of the line. (The RF loss introduced by this attenuator can be eliminated, of course, by replacing the attenuator with a reactive dc return). A high-pass filter was included to prevent photocurrent form reaching the RF detector. For the results to be described below, the on/off ratio was determined by measuring the amount of attenuation that was needed ahead of the RF detector in order to reduce the detector output level during illumination to that level measured with no illumination. In this way, detector nonlinearities were removed from the measurement.

A. Switching Characteristics

To investigate the switching performance of the device, experiments were performed over ranges in bias, RF power, and optical power level. The measured on/off ratio is shown in Fig. 7 as a function of the incident power for various bias levels. Examination of the figure shows that the switching performance improves as the bias is increased to 42 V, and then degrades as the bias is increased beyond this point. This peaking of the on/off ratio as the bias is varied, which is most pronounced at low power levels, is in qualitative agreement with the small-signal theory presented in the previous section.

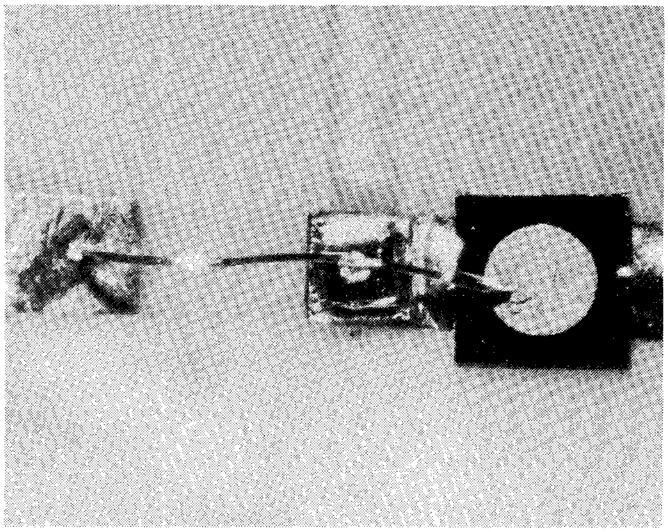

Fig. 5. Experimental microstrip configuration.

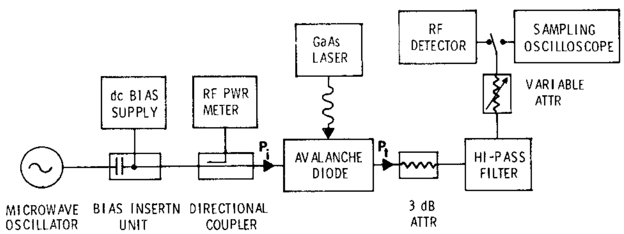

Fig. 6. Experimental apparatus.

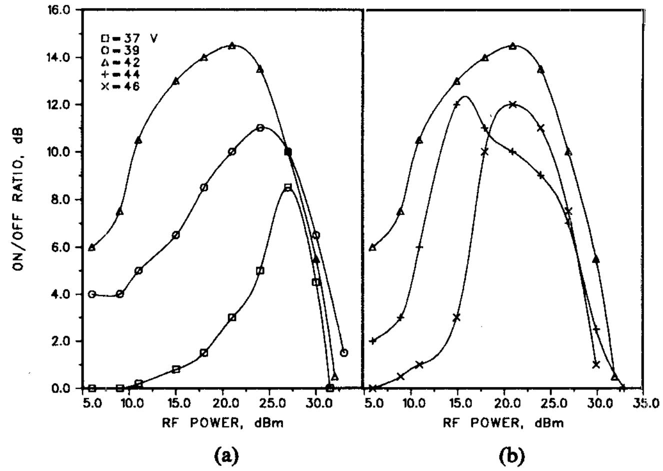

Fig. 7. Variation of the on/off ratio with RF power level for (a) various biases up to the optimum level of 42 V, and (b) various biases continuing beyond the optimum level. The optical power density was 30 W/cm^2.

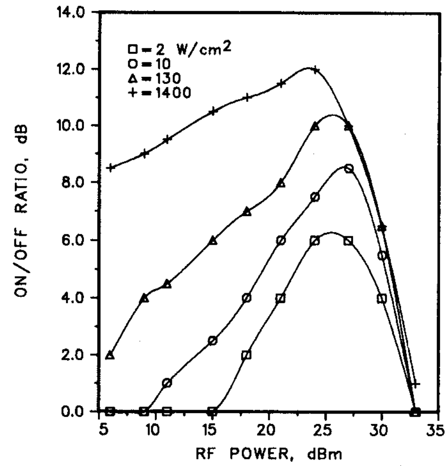

Fig. 8. Variation of the on/off ratio with RF power level for various optical-signal levels.

Fig. 7 also shows that the switching performance gradually improves with increasing RF power, and then rapidly degrades as the power level reaches 30 dBm. The maximum on/off ratio, 15 dB, occurs at 20 dBm for the 42-V bias. The on-state insertion loss at this point was 2 dB. On/off ratios as high as 20 dB have been observed for incident power levels greater than 30 dBm. However, the insertion loss for these cases was considerably higher (~8 dB).

The peaking of the on/off ratio with RF power variation was found to be dependent on the intensity of the controlling optical signal. This behavior is illustrated in Fig. 8 for a device similar to that of Fig. 7, but having a somewhat lower on/off ratio. It can be seen that the variation in on/off ratio with RF power is reduced markedly at high-illumination levels. This reduced sensitivity to RF power level is of importance for applications requiring the gating of signals of varying amplitude.

Variations in the on/off ratio with RF power level are the result of nonlinear changes in the carrier dynamics with increasing RF amplitude not accounted for in Section II. An explanation for the increase in on/off ratio with increasing RF power seen at moderate power levels awaits a more rigorous large-signal theory. However, the drop in on/off ratio seen at higher power levels can be explained quite simply by an increase in carrier multiplication at high amplitudes. When the RF swing is large, an increase in the average multiplication (over the RF cycle) is expected due to the rapid increase in multiplication with electric field. At high-power levels, the impedance for both switching states will, therefore, drop to low values, resulting in degraded switching performance. This explanation is corroborated by increased dc and decreased off-state isolation (ratio of transmitted to incident power for no illumination) observed experimentally at high-power levels.

B. Switching Speed

The switching speed of the device in response to 8-ns optical pulses was examined by directly measuring the

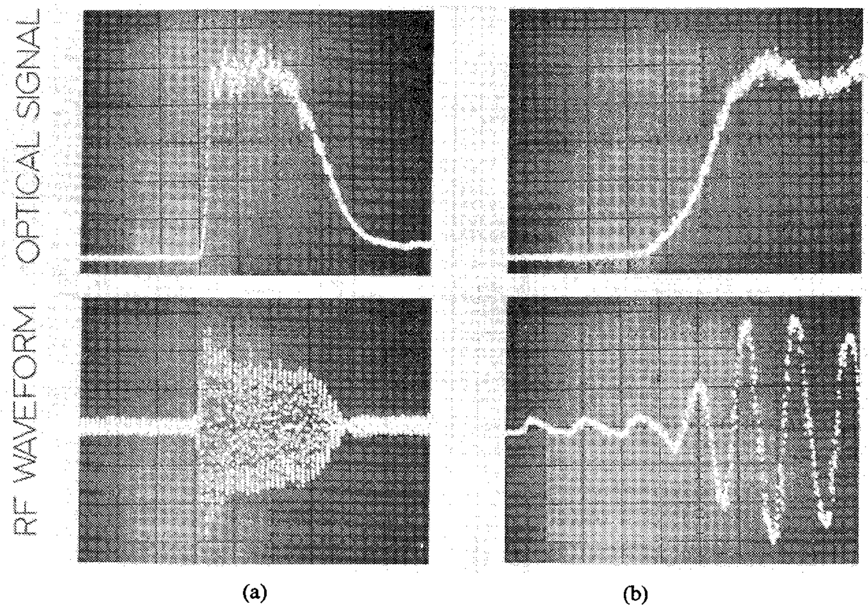

Fig. 9. (a) Optical signal and resultant RF waveform. Scale: 2 ns/div. (b) Expanded scale during the off-to-on switching transient. Scale: 0.2 ns/div.

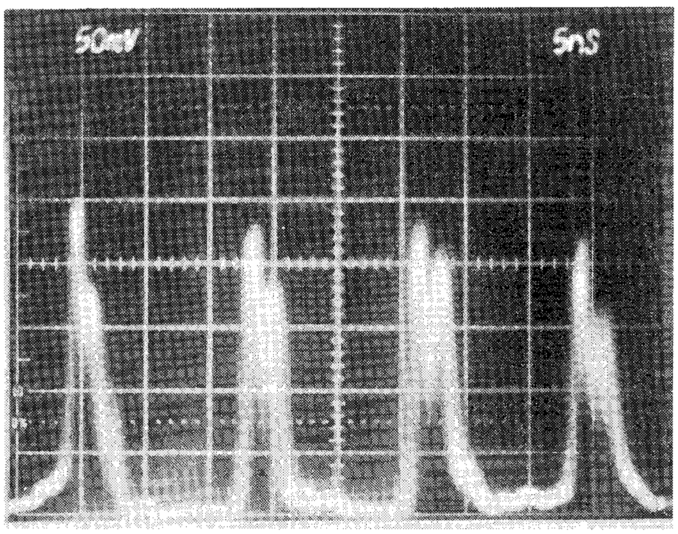

Fig. 10. Detected RF power demonstrating switching in response to a short train of optical pulses. Scale: 5 ns/div.

output RF waveform using a 12-GHz sampling system. Measured waveforms and the controlling optical signals, as monitored on a high-speed silicon photodiode, are shown in Fig. 9. Examination of the figure reveals that the rise and fall of the RF envelope occurs within 0.3 and 2 ns, respectively, and thus follows the rise and fall of the optical pulse itself.

The data-rate (or repetition-rate) capability of the device was also examined. This was done by illuminating the device with a short train of 3-ns optical pulses spaced 10 ns apart. The detected RF power is shown in Fig. 10. Differences in the shapes and amplitudes of the pulses shown in Fig. 10 are the result of differences among the controlling optical pulses. Likewise, ringing was found to be caused by ringing in the optical pulses. Hence, the results in Fig. 10 demonstrate that the data-rate capability for the device is at least 75 Mbit/s, the limit of the laser modulator.

IV. Ultimate Performance and Advantages over Other Devices

The experimental results presented here serve to demonstrate the switching characteristics and speed of this device. A considerable improvement in performance can be expected with optimized structures. In particular, an improvement of the power handling capacity should be possible with longer high-field regions since this will lower the amplitude of the ac fields. The increased impedance for longer regions can be offset by an increase in the diode's active area, which will also improve the diode's power dissipation. Although power dissipation was not the limiting factor in these experiments (the lowered ionization rate caused by a temperature rise would produce a decrease, rather than the observed increase, in operating current at high-RF-power levels), it could be an important factor in long devices. In addition to the use of a large active area and good heat-sinking techniques, a "clamping" of the supply current by the use of a high source resistance would be helpful for minimizing thermally induced changes.

The switching times as well as the data rate achieved in these experiments have been limited only by the capabilities of the present laser modulator. Because of the dc bias field, the carrier velocities remain nearly saturated throughout all stages of device operation. Hence, the switching speed is ultimately limited by the transit time of carriers through the device at the saturated drift velocity. Note that this gives rise to a basic speed advantage over conventional diode switches, in which the carrier velocities are far below saturation during substantial portions of the switching transients.

In order to approach the transit-time limit, the electric field distribution must be tailored so that the avalanche is confined to a small fraction of the high-field region. This is because the time-constant associated with the avalanche zone can be many times longer than the transit-time of this zone, as was seen in Section II-B. When the avalanche is confined, the region outside this zone will serve as a drift region for the avalanched carriers. If the field in the drift region is high enough to maintain nearly saturated drift velocities, the RF losses introduced by this region will be small [8] and cause little degradation in the on-state transmission. The transit-time limit can also be approached by utilizing a material having greatly differing electron and hole ionization rates, such as InAs, for which the avalanche response time is greatly reduced [10].

Since the saturated drift velocity is $\sim 1 \times 10^7$ cm/s, the high-field region must be kept less than 100 μm in order to maintain subnanosecond switching in a transit-time limited device. This distance is 25 times longer than the high-field region of the devices examined here, and hence one would estimate that an improvement in the power handling capacity of almost 30 dB could be realized. Scaling our present results (optimum performance at $\sim$0.1 W), this gives a power-speed product of 100 W/ns, a value two orders of magnitude better than that of conventional diode switches [1].

In comparison with optoelectronic semiconductor-plasma switches [5], [6], avalanching optoelectronic switches sacrifice ultimate RF power handling capacity for the practical advantages of lower optical power requirements and higher repetition rates. The lower optical power requirement results from the utilization of avalanche gain, while the capability for higher repetition rates results from the rapid diode recovery obtained through the utilization of field sweep-out, rather than recombination, for carrier removal.

The maximum optical-power density utilized in the present experiments was 30 W/cm^2. Assuming a circular radiation pattern 5 mil in diameter (due to fiber coupling to a 5-mil diameter device) and a dc-to-optical conversion efficiency of 1 percent (typical of semiconductor lasers), the "prime power" requirement of the present design is about 0.4 W. While this is already a quite reasonable level, substantial improvement could be obtained with top-illuminated structures in which the photon-absorption depth has been matched to the active region thickness.

V. Conclusions

An avalanching optoelectronic microwave switch has been described, and experimental results for preliminary device designs have been reported. The results demonstrate that high-speed switching with a high on/off ratio is possible with this device. Specifically, on/off ratios as high as 20 dB with on-to-off switching times of 0.3 and 2 ns, respectively, have been achieved. The demonstrated switching times, as well as the data rate (75 Mbit/s), have been limited only by the speed of the present laser modulator, and considerably higher speeds are ultimately expected to be possible. The best overall performance of the present devices has been obtained for incident power levels on the order of 0.1 W. However, substantial improvement in the power handling capacity is expected for properly designed diodes.

Due to fundamental advantages in its switching mechanism, this device is capable of higher switching speeds than conventional diode switches. It also offers the further advantage of virtually complete isolation between RF and modulator circuitry. In addition, the avalanching optoelectronic switch has practical advantages over other optoelectronic switching devices in terms of lower optical power requirements and higher repetition rates.

While further work is still needed, the results presented here encourage us to believe that this device could provide a useful means for switching moderate levels of microwave power at high speeds.

Acknowledgment

The author wishes to express his thanks to R. J. Chaffin and E. P. EerNisse for useful discussions, and to R. E. Hibray for his work in the preparation of experimental devices.

References

[1] R. V. Garver, "PIN diode switches—Speed vs. power," *Microwave J.*, vol. 21, pp. 53–58, Feb. 1978.

[2] R. A. Kiehl and E. P. EerNisse, "Improvement of TRAPATT performance with optically generated carriers," in *1976 IEEE Electron Devices Meeting, Tech. Dig.*, pp. 98–101, Dec. 1976.

[3] R. A. Kiehl and E. P. EerNisse, "Narrow microwave pulse generation by optical enhancement of TRAPATT oscillations," in *1977 IEEE Electron Devices Meeting, Tech. Dig.*, pp. 103–106, Dec. 1977.

[4] H. W. Yen, M. K. Barnoski, R. G. Hunsperger, and R. T. Melville, "Switching of GaAs IMPATT diode oscillator by optical illumination," *Appl. Phys. Lett.*, vol. 31, pp. 120–122, July 1977.

[5] A. M. Johnson and D. H. Auston, "Microwave switching by picosecond photoconductivity," *IEEE Trans. Quantum Electron.*, vol. QE-11, pp. 283–287, June 1975.

[6] W. Platte, "High-speed optoelectronic switching in silicon gap-shunt microstrip structures," *Electron. Lett.*, vol. 12, pp. 437–438, Aug. 1976.

[7] W. T. Read, "A proposed high-frequency negative-resistance diode," *Bell Syst. Tech. J.*, vol. 37, pp. 401–446, Mar. 1958.

[8] T. Misawa, "Negative resistance in p-n junctions under avalanche breakdown conditions, parts I and II," *IEEE Trans. Electron Devices*, vol. ED-13, pp. 137–143, Jan. 1966.

[9] H. Melchior, "Signal and noise response of high speed germanium avalanche diodes," *IEEE Trans. Electron Devices*, vol. ED-13, pp. 829–839, Dec. 1966.

[10] R. B. Emmons, "Avalanche-photodiode frequency response," *J. Appl. Phys.*, vol. 38, pp. 3705–3714, Aug. 1967.